Novel polyamide amidine anthraquinone platinum(II) complexes: cytotoxicity, cellular accumulation, and fluorescence distributions in 2D and 3D cell culture models

Anthony T.S. Lo, Nicole S. Bryce, Alice V. Klein, Mathew H. Todd and Trevor W. Hambley*

School of Chemistry, The University of Sydney, Camperdown 2006, NSW, Australia.

Corresponding author

Email: trevor.hambley@sydney.edu.au; Phone: +61 2 9036 9153

Abstract

1- and 1,5-Aminoalkylamine substituted anthraquinones (AAQs, 1C3 and 1,5C3) were peptide coupled to 1-, 2-, and 3-pyrrole lexitropsins to generate compounds that incorporated both DNA minor groove and intercalating moieties. The corresponding platinum(II) amidine complexes were synthesized through a synthetically facile amine-to-platinum mediated nitrile 'Click' reaction. The precursors as well as the corresponding platinum(II) complexes were biologically evaluated in 2D monolayer cells and 3D tumour cell models. Despite having cellular accumulation levels that were up to five-fold lower than that of cisplatin, the platinum complexes had cytotoxicities that were only three-fold lower. Accumulation was lowest for the complexes with two or three pyrrole groups, but the latter was the most active of the complexes exceeding the activity of cisplatin in the MDA-MB-231 cell line. All compounds showed moderate to good penetration into spheroids of DLD-1 cells with the distributions being consistent with active uptake of the pyrrole containing complexes in regions of the spheroids starved of nutrients.

Keywords

Pyrrole lexitropsins · Anthraquinone · Platinum amidine complexes · Monofunctional adducts · DNA binding · Spheroids

Introduction

Platinum complexes such as cisplatin, carboplatin, and oxaliplatin are primary components of chemotherapy for solid tumours [1-3], but they cause acute and chronic side effects and are only curative in a subset of cancers. Targeting of platinum drugs to tumour cells has the potential to overcome these limitations [4], but it has been suggested that for targeting to succeed, the drug being delivered should have a cytotoxicity of about 10 nM [5]. While the inherent potency of the existing platinum drugs might be sufficient [4], targeting is likely to be more effective if the platinum warhead being delivered is more cytotoxic because it would reduce the amount of compound that the targeting mechanism would need to deliver to cause cell death. The potential of high sequence selectivity in DNA binding for enhancing cytotoxicity is amply demonstrated by drugs such as bizelesin and adozelesin which target AT rich islands of DNA; whereas the highly successful anticancer drug cisplatin must form 14,000 adducts per genome to kill a cancer cell, these AT targeting drugs can do so with 100 adducts and perhaps as few as 2 adducts [6, 7]. Platinum complexes developed by Bierbach and colleagues that bind in the minor groove at adenine also show remarkable cytotoxicity [8, 9].

One highly effective means of introducing sequence selectivity in the binding interaction of a small molecule drug and the targeting of AT rich sequences is the use of the polyamide class of minor groove binders developed by Dervan and colleagues [10, 11]. This approach has been used successfully by Aldrich-Wright and colleagues to modify the sequence selectivity of platinum complexes [12, 13], and other groups have reported the combination of polyamides that include distamycin, netropsin, and pyrrole lexitropsins with DNA intercalators such as acridine [14-16], and bleomycin [17, 18].

We have set out to test and understand the effect of combining an intercalator motif related to those developed by Bierbach and colleagues with the polyamide motif to determine whether that generated the desired levels of cytotoxicity. To do this, we have used a 1,5-anthraquinone as a threading intercalator with the platinum moiety attached on one side and the polyamide on the other with the expectation that the polyamide preference for the minor groove would direct the platinum to the major groove, substantially enhancing the cytotoxicity. The novel polypyrrole lexitropsin anthraquinone platinum amidine class that we

developed is represented by the parent compound [PtCl(am1C3)(en)]Cl **7** and [PtCl(Py-am1,5C3)(en)]Cl **8a-c** (Scheme 1).

A further limitation of some anticancer therapeutics is that they suffer from poor tumour penetration [19]. Tumours are abnormal growths of cells with abnormal vasculature. As a result, therapeutics delivered intravenously with rapid cellular uptake will primarily impact on the tumour cells closest to the vasculature, leaving the growth of cells that are further from the vasculature largely untreated, and allowing unhindered proliferation [20]. Combining good tumour penetration with DNA damaging properties is a challenge and therefore we have also investigated the penetration of the polyamides and/or positively charged platinum complexes into spheroids as 3D models of tumours.

Results and discussion

Syntheses

Preparation of the polyamides (1-, 2- and 3-py) using Boc protected amine and methyl ester protected N-methylpyrroles using solution phase peptide synthesis and iterative coupling gave moderate yields overall (Scheme 1). Removal of the Boc group to yield the free amine was achieved with better yields by using NaOH (2 M) rather than saturated sodium hydrogen carbonate to make the solution basic after extraction with chloroform. All of the free amines of the polyamides were found to be unstable (overnight at -20 °C and under argon gas) as they readily decompose to a red coloured oil. Due to the rapid decomposition of the product, the oil was used in the peptide coupling reaction immediately to form a stable amide product. Boc removal with TFA/DCM (1:4 v/v) leads to the generation of the reactive tert-butyl cation as an intermediate which can add to the product. The addition of scavengers such as water or triisoproyplsilane (TIS) can suppress the formation of tert-butylated products. Therefore, non-anhydrous DCM was used in the removal of the Boc group.

The solution phase peptide couplings of 1C3 **2** to the polyamide carboxylic acids, **1a-c**, to form Py-1C3 conjugates, **4a-c**, was achieved in good yields and the conjugates dissolved readily in a range of organic solvents (Table 1). The Py-1,5C3 conjugates generated using solution phase peptide coupling of 1,5C3 **3** to the polyamide carboxylic acids, **5a-c**, were less

soluble than the Py-1C3 conjugates. The workup following the coupling of fluorophores (1C3 **2** and 1,5C3 **3**) entailed the extraction of the aqueous phase with copious amounts of organic solvents. The poor solubility of Py-1,5C3 conjugates, **5a-c**, in organic solvents commonly used for extraction, such as ethyl acetate and chloroform, necessitated the use of an isopropanol/chloroform (1:3 v/v) mixture. This mixture worked well for the extraction process and increased the yield of the synthesis.

Two strategies were explored for mono coupling a polyamide to the anthraquinone moiety. The first strategy was to mono Boc protect one of the amine groups followed by coupling of the polyamide, and the removal of the Boc group and basification to enable the extraction of the free amine. The second strategy was to mono couple the polyamide directly using a dropwise addition of a dilute solution of the activated polyamide carboxylic acid to a solution of 1,5C3. The latter strategy was chosen as the yields (87%) were much better than for the former strategy (7% over three steps). Di-Boc protected 1,5C3 was isolated in greater yields (45%) than the mono-Boc protected 1,5C3 using Boc anhydride despite slow addition of Boc anhydride at low temperatures. Purification of fluorophores by silica or alumina was problematic as the compounds streak on the column. Due to their high quantum yields, fluorescent impurities were difficult to separate especially when their retention factor was close to that of the product. The streaking is presumably caused by the free amine groups from the propane-1,3-diamine substituent of the anthraquinone. A few drops of ammonia (alumina chromatography) or TEA (silica chromatography) were added to the eluent to reduce streaking on the column such that purification could be improved. By reducing the number of protection and removal steps, a better yield was achieved overall by peptide coupling directly to 1C3 or 1,5C3.

Synthesis of platinum complexes

The polyamide anthraquinone amidine platinum complexes were prepared from the nitrile precursor [PtCl(en)(NCEt)]Cl **6** by the nucleophilic addition of the amine to the coordinated nitrile following procedures reported by Bierbach and colleagues [21]. All reactions proceeded well and gave acceptable yields and purities (Table 2).

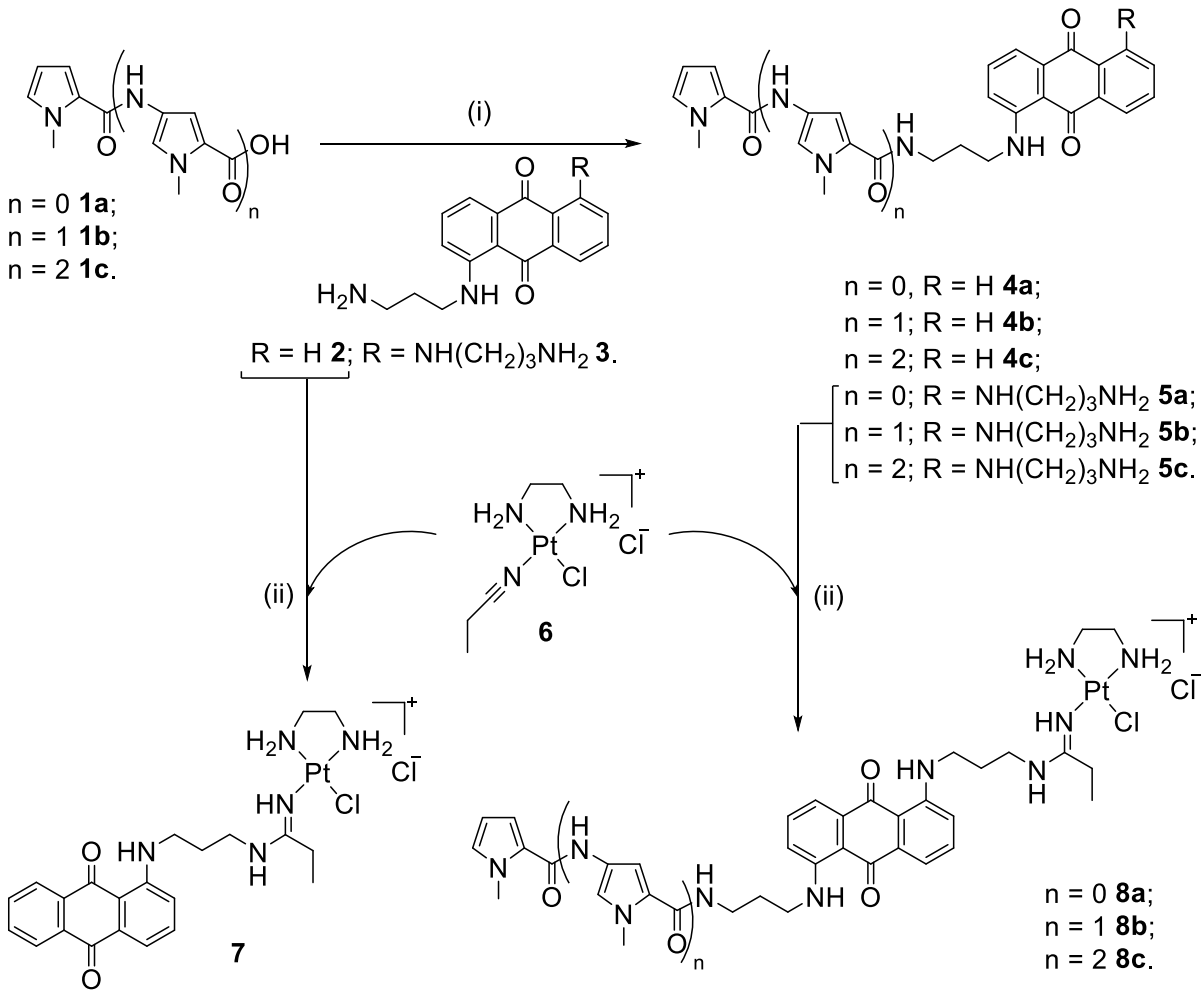

Scheme 1 Scheme for reagents and conditions employed in ligand and platinum(II) complex synthesis. i) HBTU, *N*,*N*-diisopropylethylamine, acetonitrile, rt; ii) DMF, 50 °C, 72 h.

Table 1 Generation of the polyamide-1C3 **4a-c** or polyamide-1,5C3 **5a-c** conjugates using standard coupling conditions.

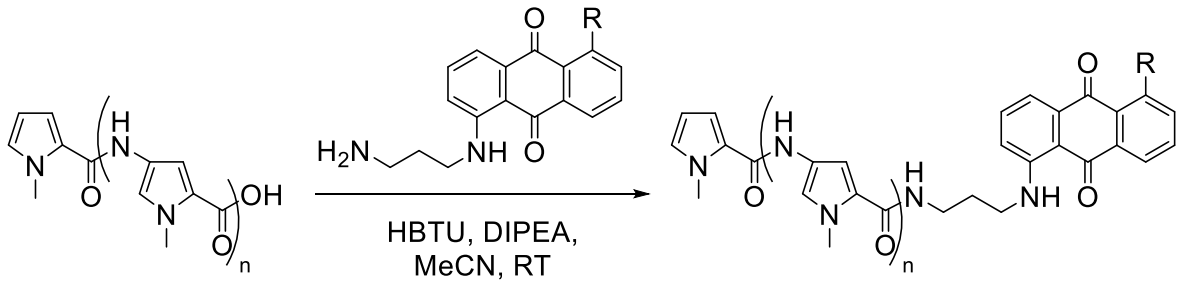

Product	R	n	Yield [%]
1py-1C3 **4a**	H	0	97
2py-1C3 **4b**	H	1	63
3py-1C3 **4c**	H	2	63
1py-1,5C3 **5a**	$NH(CH_2)_3NH_2$	0	87
2py-1,5C3 **5b**	$NH(CH_2)_3NH_2$	1	31
3py-1,5C3 **5c**	$NH(CH_2)_3NH_2$	2	23

Table 2 Generation of the [PtCl(am1C3)(en)]Cl 7 and [PtCl(Py-am1,5C3)(en)]Cl **8a-c**

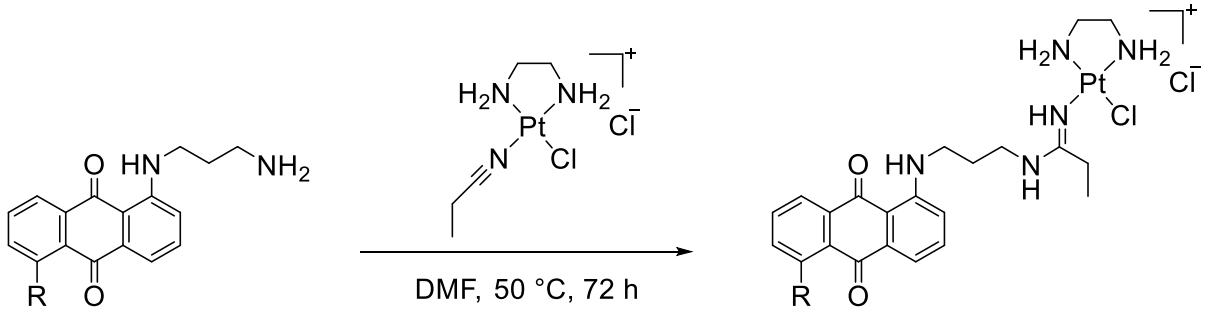

Product	R	Yield [%]
[PtCl(am1C3)(en)]Cl 7	H	41
[PtCl(1py-am1,5C3)(en)]Cl 8a	- (1py)$CONH(CH_2)_3NH$	58
[PtCl(2py-am1,5C3)(en)]Cl 8b	- (2py)$CONH(CH_2)_3NH$	40
[PtCl(3py-am1,5C3)(en)]Cl 8c	- (3py)$CONH(CH_2)_3NH$	22

In vitro cytotoxicity

The cytotoxicities of the ligands and the novel platinum complexes were evaluated in human cancer cell lines from the colon (DLD-1) and breast (MDA-MB-231). The IC_{50} values, calculated from the dose-survival curves after 72 h of incubation are summarised in Table 3. For comparison, the cytotoxicity of cisplatin was evaluated under the same conditions and yielded IC_{50} values similar to those reported previously for the two cell lines [22, 23]. The mono- and di-aminopropyl substituted anthraquinones, **2** and **3**, were similarly potent in inhibiting DLD-1 cells, but were more active against MDA-MB-231 cells than cisplatin with **3** being significantly more potent than **2** in both cell lines. Except for **5a**, all polyamide-anthraquinone compounds (**4a-c** and **5b-c)** displayed cytotoxicity lower than the 100 μM cut off in both cell lines. The platinum complexes **7** and **8a-c**, showed similar yet moderate cytotoxicity in both cell lines with the cytotoxicity increasing slightly with three pyrrole rings such that **8c** has cytotoxicity similar to that of **2**. The results suggest that the cytotoxicity can be mainly attributed to the platinum-DNA adduct formation, although the polyamide component of the compound is influencing this to a small degree.

Table 3 IC_{50} values after incubation for 72 h in DLD-1 and MDA-MB-231 cells. Values are expressed as mean ± standard error of mean (SEM) and are derived from at least 3 independent experiments.

Series	Compound	IC_{50} (μM) ± SEM	
		DLD-1	MDA-MB-231
	Cisplatin	11.2 ± 0.3	22.0 ± 0.6
Polyamide-1C3	1C3 **2**	19.8 ± 0.4	14.4 ± 0.4
	1py-1C3 **4a**	>100	>100
	2py-1C3 **4b**	>100	>100
	3py-1C3 **4c**	>100	>100
Polyamide-1,5C3	1,5C3 **3**	8.5 ± 0.5	4.3 ± 0.1
	1py-1,5C3 **5a**	24.1 ± 0.9	24.2 ± 0.7
	2py-1,5C3 **5b**	>100	>100
	3py-1,5C3 **5c**	>100	>100
Platinum(II)	[PtCl(am1C3)(en)]Cl **7**	28.9 ± 0.3	30.1 ± 0.6
	[PtCl(1py-am1,5C3)(en)]Cl **8a**	23.9 ± 0.4	29.0 ± 0.3
	[PtCl(2py-am1,5C3)(en)]Cl **8b**	29.7 ± 0.6	27.9 ± 0.4
	[PtCl(3py-am1,5C3)(en)]Cl **8c**	21.0 ± 0.5	16.2 ± 0.3

Mono-layer cellular accumulation studies of platinum(II) conjugates

To investigate the uptake of the platinum complexes in cells, mono-layer cellular accumulation studies were conducted. The cellular accumulations of the polyamide-anthraquinone conjugates tethered to the platinum(II) moiety were compared to that for cisplatin in MDA-MB-231 and DLD-1 carcinoma cells by measuring platinum levels and the results are shown in Fig. 1.

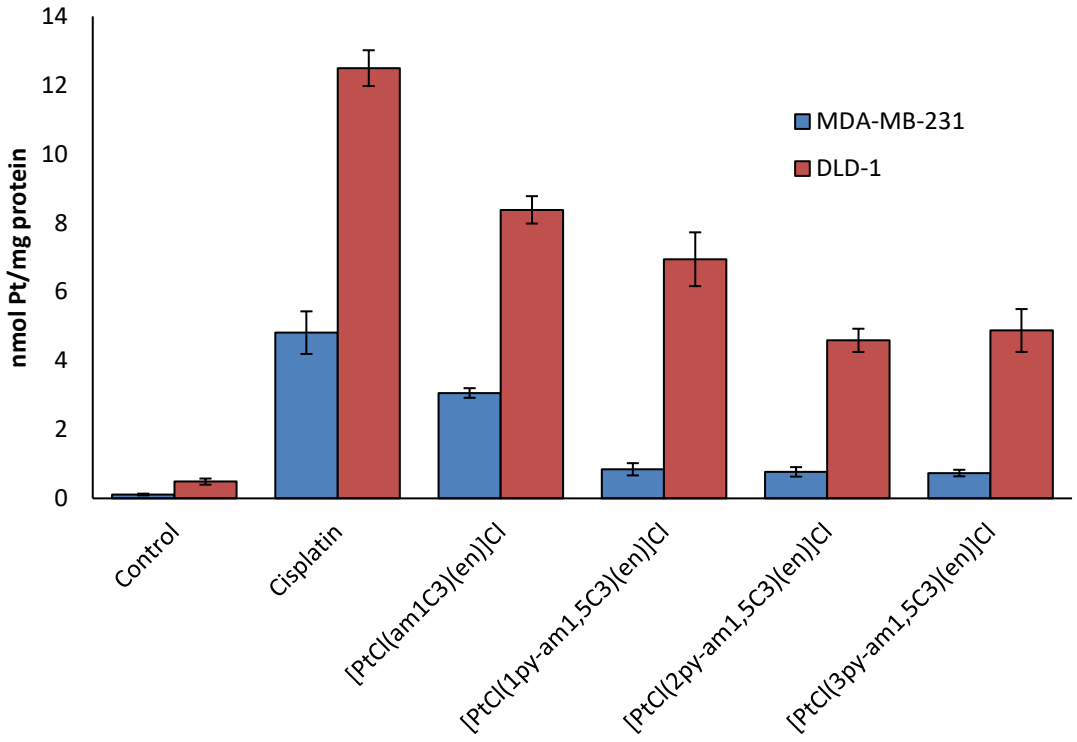

Fig. 1. Platinum accumulation in MDA-MB-231 (blue) and DLD-1 (red) carcinoma cells following 4 h treatment with 10 μM concentrations of cisplatin, [PtCl(am1C3)(en)]Cl **7**, [PtCl(1py-am1,5C3)(en)]Cl **8a**, [PtCl(2py-am1,5C3)(en)]Cl **8b**, [PtCl(3py-am1,5C3)(en)]Cl **8c**. Values were obtained from at least 3 independent experiments and error bars represent ± the standard error.

The neutral platinum complex, cisplatin, was found to accumulate more than any of the positively charged platinum complexes. Neutral complexes can passively diffuse more readily through cell membranes and were expected to enter cells more rapidly than positively charged species. The lower cellular accumulation of [PtCl(am1C3)(en)]Cl **7** and the [PtCl(Py-am1,5C3)(en)]Cl complexes **8a-c** is consistent with the positive charge hindering cellular entry.

Adding one or two polyamides to the conjugates was found to hinder cellular accumulation, but adding a third did not further reduce cellular accumulation.

It is notable that the cytotoxicities of complexes **7** and **8a-c** are similar in the two cells lines despite much higher accumulation in the DLD-1 cell line. This suggests a substantially lower sensitivity to the complexes in that line.

Fluorescence studies

The fluorescence profiles of the conjugates are shown in Fig. S27. The polyamide-1C3 conjugates **4a-c** have an excitation wavelength between 520 and 525 nm and an emission wavelength between 625 and 630 nm while the polyamide-1,5C3 conjugates **5a-c** have slightly longer excitation wavelengths between 525 and 530 nm and a shorter emission wavelength between 615 and 616 nm. The platinum(II) complexes **7, 8a-c** have similar excitation wavelengths as the polyamide-1,5C3 conjugates **5a-c**, with the emission wavelengths between 611 and 615 nm. All polyamide-anthraquinone conjugates **4a-c, 5a-c** were dissolved in DMSO whereas the platinum(II) complexes **7, 8a-c** were dissolved in DMF. This was due to the possible coordination of DMSO to the monofunctional platinum(II) complexes. The highest fluorescence intensities were obtained in organic solvents whereas fluorescence quenching was observed in phosphate buffered saline (PBS) (Fig. S27).

Chromophores such as AAQs are reported to be influenced by intermolecular hydrogen bonding interactions in the excited state with polar aprotic solvents that can emit strong fluorescence [24], whereas the fluorescence of the chromophores in polar protic solvents such as water or alcohol is usually quenched or dampened [25]. The fluorescence quenching of these AAQs tethered to polyamides and/or platinum(II) complexes is consistent with these reports.

DNA quenching studies

Fluorescence quenching of intercalating agents containing platinum complexes in the presence of DNA has been reported in the literature [26]. Quenching studies of the anthraquinone tethered compounds and their platinum complexes were used to establish whether the fluorescence of the compounds was quenched upon interaction with DNA. Ethidium bromide (EtBr) was used as a control in this study as this intercalator is known to be fluorescent upon

intercalating with DNA. In this study, fluorescence of each of **2, 4a-c** and **3** was observed following intercalation in DNA (Fig. 2). As DNA intercalation is reversible, EtBr may have a greater affinity for DNA and displace **2, 4a-c**. In contrast, Py-1,5C3 **5a-c** and platinum(II) complexes **7, 8a-c** were quenched upon intercalation with DNA (Fig. 2). The results suggested that the fluorescence of the anthraquinone moiety can be quenched by DNA and consequently localisation at the nucleus may not be observed [26].

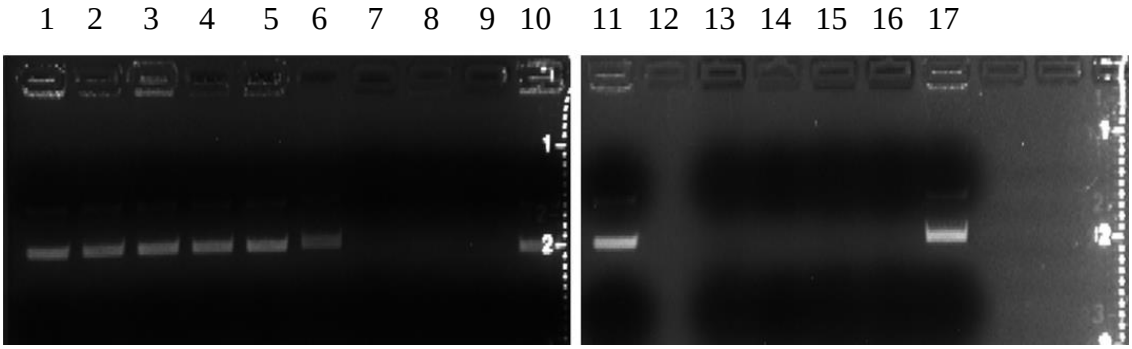

Fig. 2. Fluorescence quenching of AAQs with pBr322 DNA. A 1.0% agarose gel showing the electrophoretic mobility of pBr322 DNA which has been treated with compounds (5 μM) in TE buffer for lanes 1-17: (1) TE, (2) 1C3 **2**, (3) 1py-1C3 **4a**, (4) 2py-1C3 **4b**, (5) 3py-1C3 **4c**, (6) 1,5C3 **3**, (7) 1py-1,5C3 **5a**, (8) 2py-1,5C3 **5b**, (9) 3py-1,5C3 **5c**, (10) EtBr, (11) TE, (12) Blank, (13) [PtCl(am1C3)(en)]Cl **7**, (14) [PtCl(1py-am1,5C3)(en)]Cl **8a**, (15) [PtCl(2py-am1,5C3)(en)]Cl **8b**, (16) [PtCl(3py-am1,5C3)(en)]Cl **8c**, (17) TE.

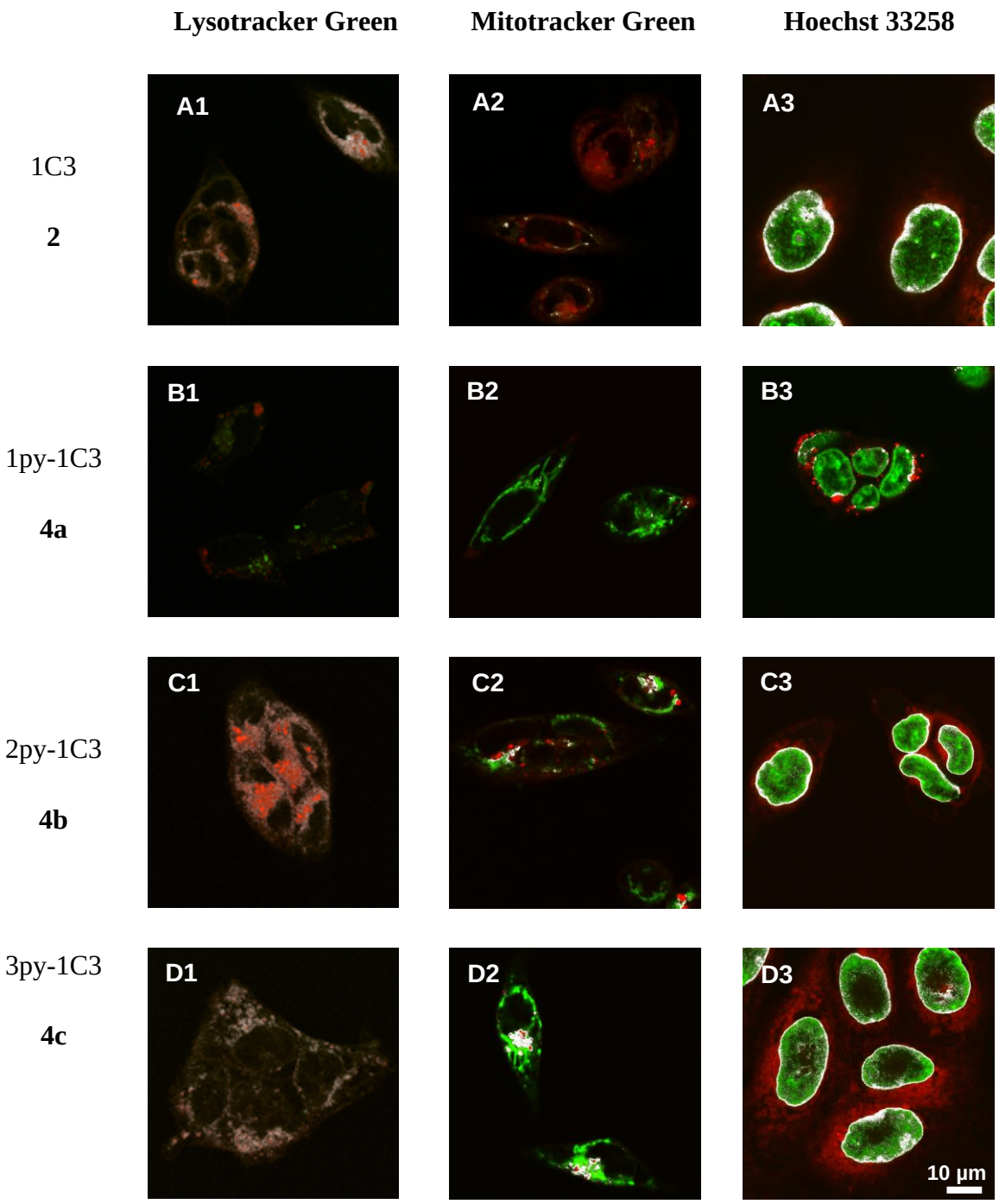

Fig. 3. Representative fluorescence images of monolayer DLD-1 colorectal cancer cell culture after 4 h incubation with the polyamide-1C3 series (10 µM) (red) and 5 min incubation with (1) Lysotracker green (green, left), (2) Mitotracker green (green, middle) and (3) Hoechst 33258 (green, right) prior to imaging. All images were taken from the middle plane of live monolayer culture. Colocalised colours are indicated in white. Scale bar represents 10 µm.

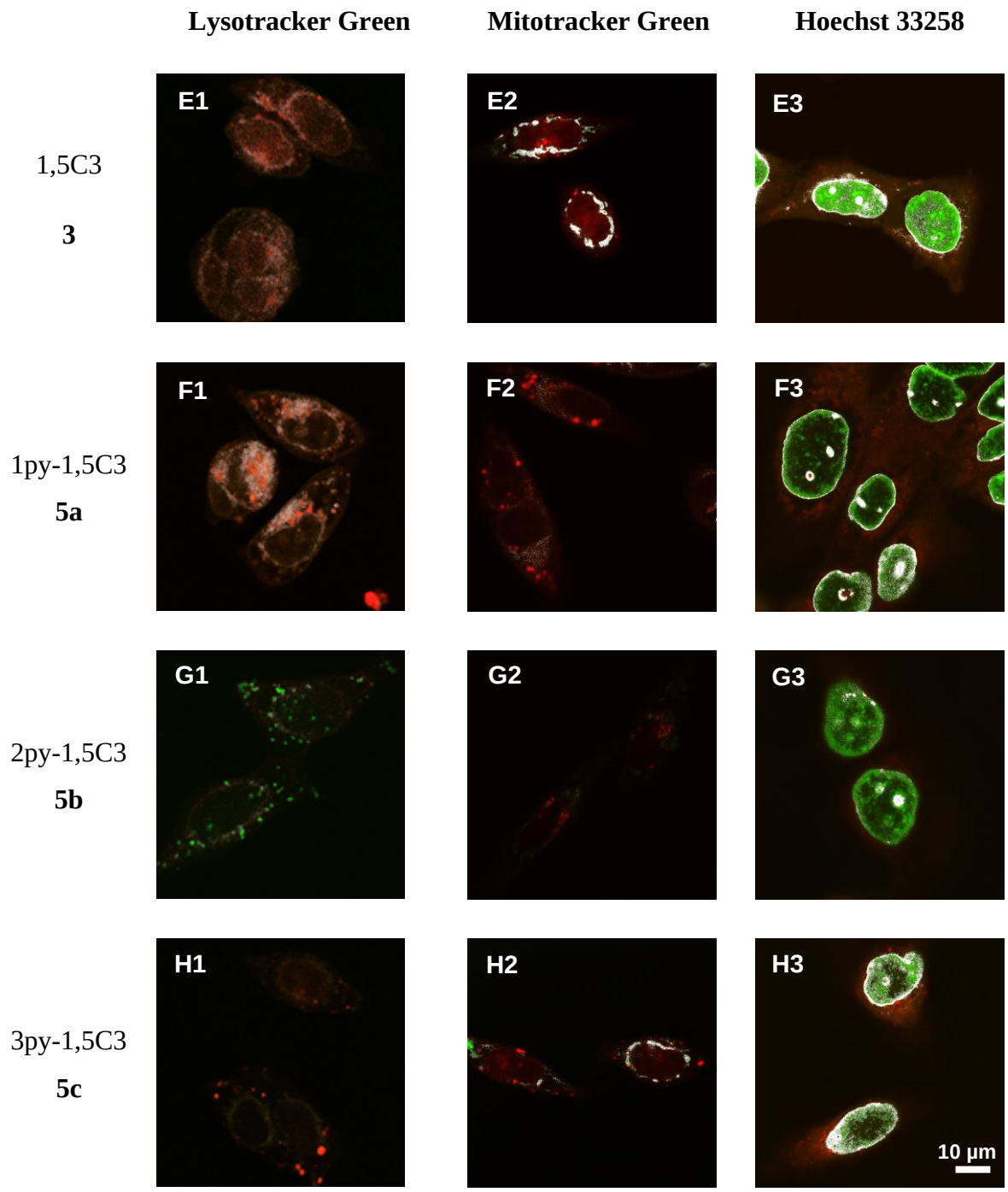

Fig. 4. Representative fluorescence images of monolayer DLD-1 colorectal cancer cell culture after 4 h incubation with the polyamide-1,5C3 series (10 µM) (red) and 5 min incubation with (1) Lysotracker green (green, left), (2) Mitotracker green (green, middle) and (3) Hoechst 33258 (green, right) prior to imaging. All images were taken from the middle plane of live monolayer culture. Colocalised colours are indicated in white. Scale bar represents 10 µm.

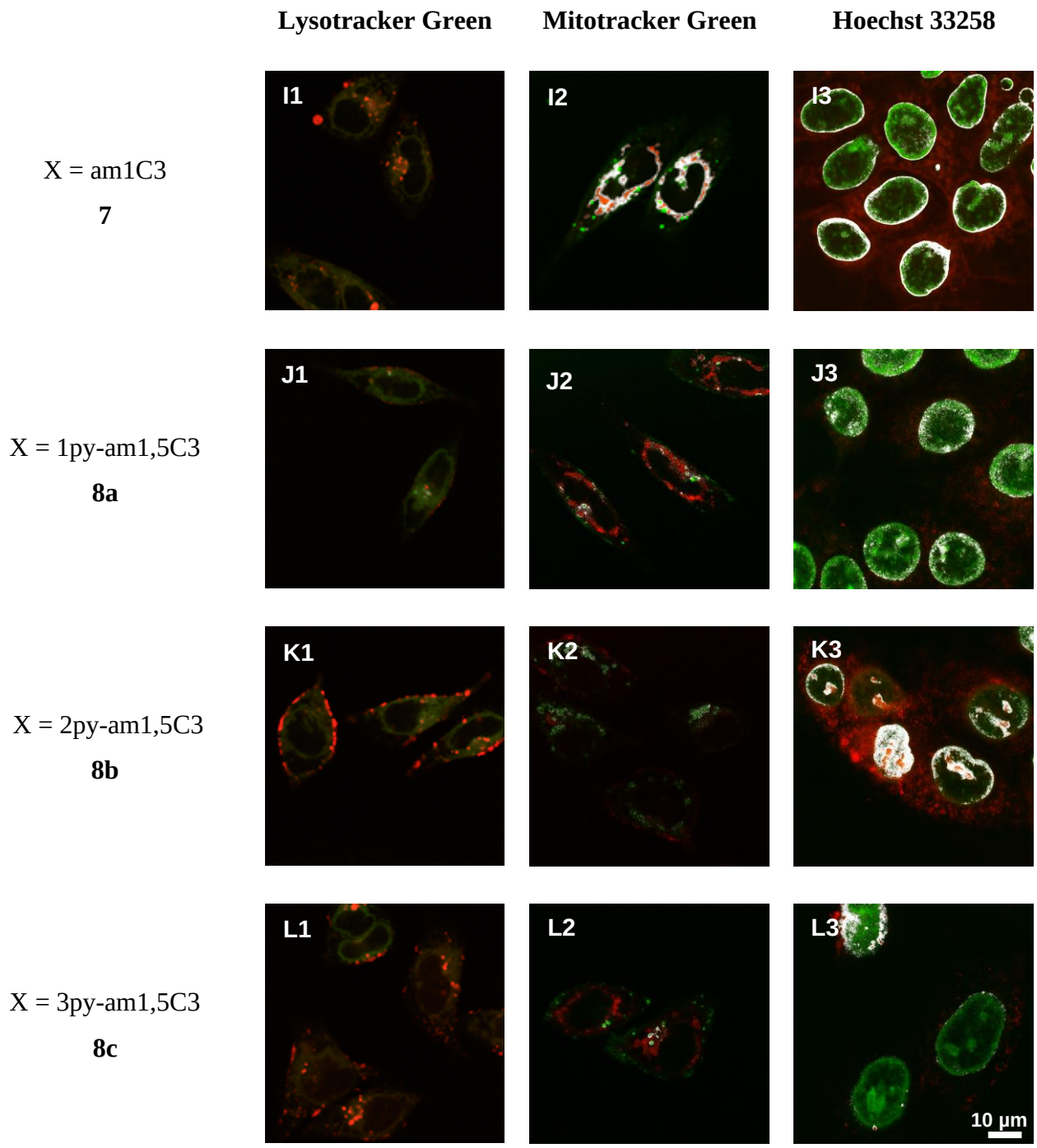

Fig. 5. Representative fluorescence images of monolayer DLD-1 colorectal cancer cell culture after 4 h incubation with the [PtCl(X)(en)]Cl series (10 µM) (red) and 5 min incubation with (1) Lysotracker green (green, left), (2) Mitotracker green (green, middle) and (3) Hoechst 33258 (green, right) prior to imaging. All images were taken from the middle plane of live monolayer culture. Colocalised colours are indicated in white. Scale bar represents 10 µm.

Subcellular distribution studies

Fluorescence arising from the polyamide-1C3 conjugates (**4a-c**) was seen throughout the cytosol and appeared to be most strongly co-localised with the lysosomes which may indicate that the compounds are degraded inside the cell (Fig. 3). Fluorescence is also seen around the nuclear membrane. Similarly, for the polyamide-1,5C3 conjugates **5a-c**, the compounds co-localised with the lysosomes and around the nuclear membrane. There is also strong fluorescence seen in the nucleoli (Fig. 4).

Fluorescence due to $[PtCl(am1C3)(en)]^+$ **7** was particularly strong in the mitochondria as well as around the nuclear membrane (Fig. 5). Mitochondrial accumulation is expected for a lipophilic cation such as this. The fluorescence of the cells treated with the complexes in the pyrrole-1,5C3-Pt(II) series **8a-c** was significantly less intense than seen in those treated with **7** which is consistent with the lower cellular accumulation for these compounds. As a result, the parameters such as laser power, gain and slit width were increased to obtain the fluorescence images for cells treated with **8a-c** (Fig. 5). With the parameters of image collection changed for the [PtCl(Py-am1,5C3)(en)]Cl complexes **8a-c**, untreated cells were also imaged as controls. Cell autofluorescence was not observed despite higher laser power being used suggesting that the red fluorescence with the new parameters can be attributed to the anthraquinone tethered platinum complexes. For the pyrrole-1,5C3-Pt(II) series, fluorescence was most visible on the edges of the nuclei, similar to that seen for the polyamide-1C3 and polyamide-1,5C3 compounds. Low level fluorescence was also seen throughout the cytosol, but with less evidence of co-localisation with the lysozomes. Other positively charged compounds such as $[Pt(dien)1,5C3]^{2+}$ [27] and doxorubicin have also been seen localised in the nucleoli [28], but less so in other regions of the nucleus. This may arise because damping of fluorescence by DNA occurs elsewhere in the nucleus, but not in the nucleolus. Despite the lack of fluorescence in the nucleus, the anthraquinone platinum complexes were inferred to form lesions with DNA that contributed to the cytotoxicity of the complexes.

Fluorescence distribution studies in HRE-EosFP transfected DLD-1 spheroids

1C3 was shown to diffuse poorly into spheroids with the highest fluorescence seen at the periphery of the spheroid (Fig. 6) as reported previously [20]. The fluorescence intensity falls to 50% of the peak value at less than 20 μm into the spheroid, consistent with rapid uptake by the cells on the periphery. In contrast, the conjugates with 1C3 tethered to polyamides (**4a-c**),

diffused substantially further into the spheroid with 50% intensity reached at from 50 to 150 µm into the spheroid (Fig. 6). Curiously, **4b** which has two pyrrole groups diffuses furthest. 1,5C3 and the polyamide compounds derived from it, all diffuse into spheroids to similar extents with 50% intensity reached at from 40 to 60 µm (Fig. 6).

When polyamides were tethered to the positively charged anthraquinone-platinum(II) complex, the fluorescence of the compound decreased. The fluorescence could not be detected using the same parameters and therefore the slit width, laser power, and the gain were increased. Consequently, the fluorescence intensities of the polyamide-anthraquinone-platinum(II) complexes cannot be directly compared to those for the anthraquinone-platinum(II) complex or the polyamide-anthraquinone conjugates. The [PtCl(Py-am1,5C3)(en)]Cl series (**8a-c**) diffused into the spheroids to similar extents and less than the conjugates not bound to platinum, with 50% intensity reached at about 30 to 50 µm from the periphery of the spheroid. Complex **7**, diffused furthest into the spheroids, reaching 50% intensity at about 130 µm. This is surprising since it was taken up more readily by DLD-1 cells in 2D culture and may indicate that the pyrrole containing compounds are taken up via other pathways when the cells are in 3D cultures. We have recently reported that cells in the hypoxic region of spheroids are particularly effective at taking up a glucose tagged fluorophore, which is consistent with selective expression of GLUT transporters in this region [29]. While these seem unlikely candidates for transport of the pyrrole containing compounds, the cells beyond the periphery of the spheroids are starved of most nutrients and are likely to express a range of transporters to address the resulting deficiencies.

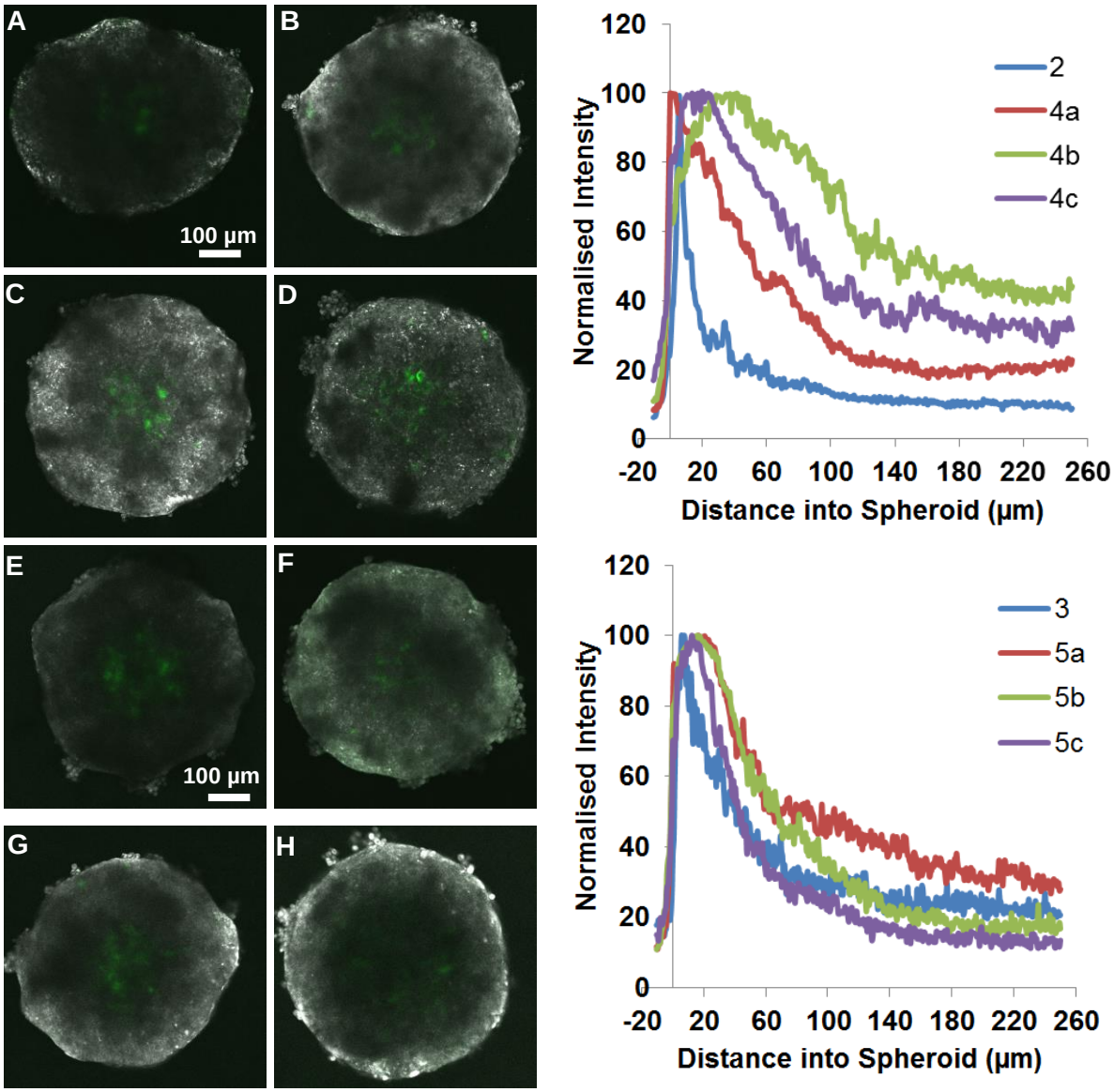

Fig. 6. Left: Representative fluorescence images of medium size (15K cells) HRE-EosFP transfected DLD-1 colorectal cancer cell spheroids after 24 hr incubation with the compounds (10 µM) (white) and HRE-EosFP (green); (A) 1C3 **2**, (B) 1py-1C3 **4a**, (C) 2py-1C3 **4b**, (D) 3py-1C3 **4c**, (E) 1,5C3 **3**, (F) 1py-1,5C3 **5a**, (G) 2py-1,5C3 **5b**, (H) 3py-1,5C3 **5c**. All images were taken from the middle plane of live whole spheroids using 2× zoom. R**ight:** Fluorescence distribution profiles of HRE-EosFP transfected DLD-1 colorectal cancer cell spheroids with compounds grouped by series. Profiles were obtained by the average fluorescence profiles of 360 lines drawn from the background (-10 µm) away from the periphery to the centre of the spheroid and normalised against the maximum edge fluorescence intensity. At least three spheroids from three independent experiments were used to create each profile.

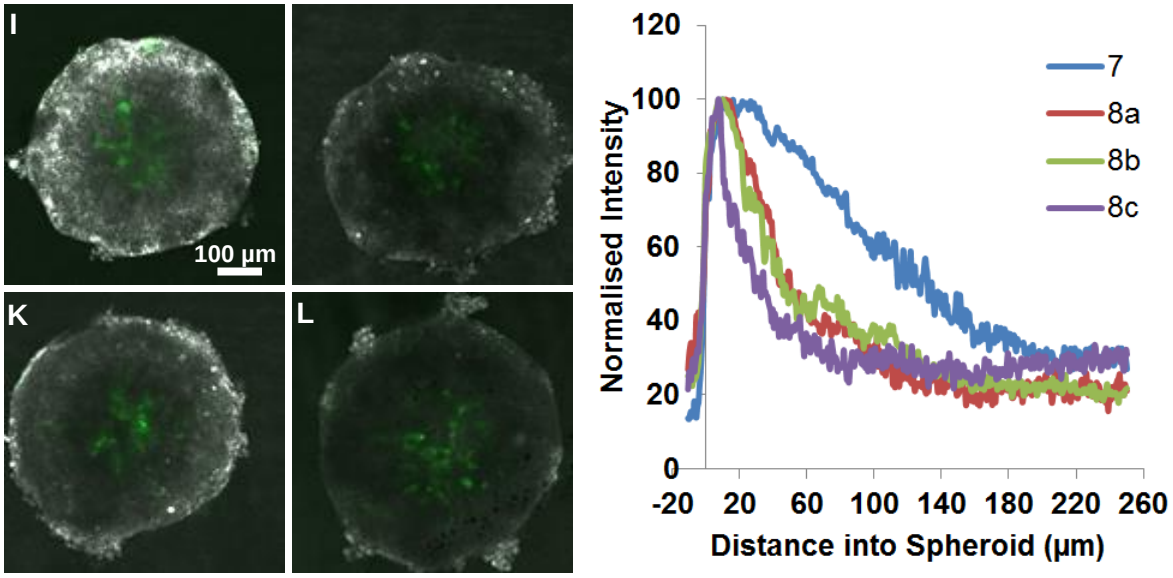

Fig. 7. **Left:** Representative fluorescence images of medium size (15K cells) HRE-EosFP transfected DLD-1 colorectal cancer cell spheroids after 24 h incubation with the compounds (10 µM) (white) and HRE-EosFP (green); (I) [PtCl(am1C3)(en)]Cl **7**, (J) [PtCl(1py-am1,5C3)(en)]Cl **8a**, (K) [PtCl(2py-am1,5C3)(en)]Cl **8b**, (L) [PtCl(3py-am1,5C3)(en)]Cl **8c**. All images were taken from the middle plane of live whole spheroids using 2× zoom. **Right:** Fluorescence distribution profiles of HRE-EosFP transfected DLD-1 colorectal cancer cell spheroids with compounds grouped by series. Profiles were obtained by the average fluorescence profiles of 360 lines drawn from the background (-10 µm) away from the periphery to the centre of the spheroid and normalised against the maximum edge fluorescence intensity. At least three spheroids from three independent experiments were used to create each profile.

Conclusions

In this work, we have described the synthesis and biological evaluation of novel hybrid polyamide-AAQ conjugates and polyamide-AAQ platinum(II) complexes designed with minor groove binding, intercalating, and major groove binding components. These compounds were expected to be substantially more potent than existing platinum complexes, but this has proved not to be the case. We have separately investigated in detail, the DNA binding profiles of these compounds and have reached the conclusion that it is the formation of the Pt-N7 adducts, particularly on guanine, that determine where and how the complexes bind to DNA [30]. This was unexpected because the other modes of interaction, minor groove binding of the polyamide component and intercalation of the anthraquinone, are non-covalent and equilibration is expected on a much more rapid timescale than formation of the coordinative bond to DNA. This has very likely contributed to the cytotoxicity of these complexes being lower than anticipated. However, the fact that the pyrrole coupled platinum

complexes can kill cells despite substantially lower uptake suggests that they are inherently more potent (on a per platinum in the cell basis) and therefore may be suitable for targeting of cancer cells by nutrient transporters such as PSMA or the folate receptor. Pyrrole coupled versions of more active analogues such as the acridine compounds investigated by Bierbach and colleagues [9, 21] could hold even more promise. Also, uncharged analogues are likely to exhibit better uptake and would also be worthy of investigation.

Cell accumulation and distribution studies show that the uptake of the platinum complexes is negatively impacted by the presence of the pyrroles and that they are distributed in parts of the cell that may contribute less to the cytotoxic effects. Despite the polyamides not contributing as expected to the cytotoxicity, their incorporation resulted in changes in the extent of penetration into spheroids, which is another feature that would likely provide advantages in a clinical context.

Experimental

All commercial reagent grade chemicals were used without further purification. Polyamides **1a-c** [31], aminoalkyl anthraquinones **2** [32] and **3** [33], and [PtCl(en)(NCEt)]Cl **6** [8] were prepared according to reported procedures and details are provided in the Supporting Information along with NMR spectra. The spectroscopic data were consistent with data reported in the literature.

cis-Diamminedichloridoplatinum(II), ethidium bromide (EtBr), bromophenol blue, DMF, and sodium acetate were purchased from Sigma-Aldrich, Pty., Ltd, Australia. Absolute ethanol, and EDTA were purchased from Ajax Chemicals, Australia.

Physical measurements

^{1}H and ^{13}C Nuclear Magnetic Resonance (NMR) spectroscopy was performed at 300 K on a Bruker Avance DPX 200 MHz spectrometer or a Bruker AMX 300, 400 or 500 MHz spectrometer. Commercially available deuterated solvents were used and internal references were made using isotopic impurities. Signals were reported in the order of chemical shift (ppm downfield with respect to internal standard TMS), followed by the multiplicity, integration, coupling constants *J* (Hz) and assignments. ^{195}Pt NMR spectroscopy was performed at 300 K

using a Bruker AMX 400 or 500 MHz spectrometer. The chemical shifts were referenced to an external standard, $K_2[PtCl_4]$, in D_2O (-1620 ppm) before obtaining the spectra. Low-resolution mass spectrometry (MS) was performed by electrospray ionization (ESI) using a Finnigan LCQ ion trap spectrometer and high-resolution mass spectrometry (HRMS) was performed on a VG Autospec mass spectrometer operating at 70 eV.

Preparation of polyamide-1C3 4a-c

To a solution of polyamide carboxylic acid **1a-c** (6.5 mmol, 1.0 eq) in anhydrous DCM (5 mL) was added DIPEA (3.0 eq). 1C3 **2** (1.1 eq), EDC·HCl (1.2 eq) and HOB*t* (1.2 eq) were added to the reaction and stirring was continued for 12 h at rt under N_2. Water was added to the reaction and the aqueous phase was carefully acidified using HCl (1 M) until pH 3 and extracted with DCM (3 × 25 mL). NaOH (1 M) was added dropwise to the aqueous layer until pH 10 was reached and extracted with DCM (3 × 25 mL). The combined organic phases were dried (Na_2SO_4) and concentrated under reduced pressure.

Preparation of polyamide-1,5C3 5a-c

To a solution of polyamide carboxylic acid **1a-c** (6.5 mmol, 1.0 eq) in anhydrous DMF (5 mL) was added DIPEA (3.0 eq). 1,5C3 **3** (1.1 eq) and HBTU (1.2 eq) were added to the reaction and stirring was continued for 12 h at rt under N_2. Water was added to the reaction and the aqueous phase was carefully acidified to pH 3 using HCl (1 M) and washed with chloroform (3 × 100 mL). NaOH (1 M) was added dropwise to the aqueous layer until pH 10 was reached and extracted with isopropanol/chloroform mixture (1:3 v/v, 3 × 200 mL). The combined organic phases were dried (Na_2SO_4) and concentrated under reduced pressure.

Preparation of [PtCl(am1C3)(en)]Cl 7 and [PtCl(Py-am1,5C3)(en)]Cl 8a-c

To a solution of 1C3 **2** or polyamide-1,5C3 compounds **5a-c** (0.22 mmol, 1.0 eq) in anhydrous DMF (5 mL) was added [PtCl(en)(NCEt)]Cl **6** (0.22 mmol, 1.0 eq). The reaction mixture was heated at 50 °C and stirring was continued for 72 h [8]. The mixture was filtered through a hydrophobic membrane filter into anhydrous diethyl ether (400 mL) dropwise and was stirred vigorously for 2 h. The purple solid was removed by filtration and washed with cold anhydrous chloroform (300 mL) followed by washing with anhydrous diethyl ether (100 mL). The solid was air dried for 15 min and dried *in vacuo* in a desiccator.

***N*-(3-(9,10-dioxo-9,10-dihydroanthracen-1-ylamino)propyl)-1-methyl-1*H*-pyrrole-2-carboxamide (1py-1C3) 4a**

The peptide coupling of methylpyrrole carboxylic acid (50 mg, 0.4 mmol, 1.0 eq) and 1C3 2 (123.3 mg, 0.44 mmol, 1.1 eq) followed general procedure A yielding **4a** (149.7 mg, 97%) as a red solid; **M.p.** 147-148 °C; **IR** (ATR) 3406, 2954, 2880, 1677, 1630, 1593, 1510, 1317, 1270 cm^{-1}; **^{1}H NMR** (300 MHz, $CDCl_3$) δ 9.81 (1H, br s), 8.20-8.40 (2H, m), 7.66-7.88 (3H, m), 7.50-7.66 (2H, m), 7.05-7.15 (1H, m), 6.66-6.72 (1H, m), 6.49-6.54 (1H, m), 5.98-6.10 (2H, m), 3.93 (3H, s), 3.54-3.66 (2H, m), 3.42-3.54 (2H, m), 2.0-2.2 (2H, m); **^{13}C NMR** (75 MHz, $CDCl_3$) δ 185.0, 183.6, 162.0, 151.5, 137.6, 135.2, 134.8, 134.5, 133.8, 132.9, 132.8, 127.8, 126.6, 125.5, 117.6, 115.7, 113.0, 111.3, 107.0, 40.6, 37.1, 36.5, 29.3; **MS** (ESI +ve) m/z 388.0 ($2M+Na^+$, 100%); **HRMS** (ESI +ve) calcd for $C_{23}H_{22}N_3O_3^+$ 388.16612 found 388.16621.

***N*-(3-(9,10-dioxo-9,10-dihydroanthracene-1-ylamino)propyl)-1-methyl-4-(1-methyl-1*H*-pyrrole-2-carboxamido)-1*H*-pyrrole-2-carboxamide (2py-1C3) 4b**

The peptide coupling of methylpyrrole polyamide carboxylic acid (0.158 g, 0.64 mmol, 1.0 eq) and 1C3 **2** (0.197 g, 0.70 mmol, 1.1 eq) followed general procedure A. The residue was purified by flash column chromatography (1:1 v/v, EtOAc/hexane, R_F 0.08) yielding **4b** (0.206 g, 63%) as a red solid; **M.p.** 114-116 °C; **IR** (ATR) 3355, 3010, 2953, 2862, 1632, 1592, 1510, 1415, 1272 cm^{-1}; **^{1}H NMR** (400 MHz, $CDCl_3$) δ 9.81 (1H, br s), 8.20-8.30 (2H, m), 7.50-7.80 (5H, m), 7.30-7.36 (2H, m), 7.05-7.11 (2H, m), 6.74-6.78 (1H, br s), 6.58-6.60 (1H, m), 6.50-6.57 (1H, m), 6.08-6.18 (1H, m), 5.80-6.08 (1H, m), 3.95 (3H, s), 3.89 (3H, s), 3.54-3.62 (2H, m), 2.42- 3.52 (2H, m), 2.0-2.15 (2H, m); **^{13}C NMR** (75 MHz, $CDCl_3$) δ 184.2, 183.3, 161.6, 159.0, 150.9, 134.7, 134.3, 133.8, 133.5, 132.5, 132.3, 128.0, 126.2, 126.1, 125.1, 122.7, 121.4, 118.7, 117.3, 115.3, 112.3, 111.8, 107.0, 103.0, 40.0, 36.8, 36.5, 36.3, 28.7; **MS** (ESI +ve) m/z 510.1 ($M+H^+$, 83%), 532.1 ($M+Na^+$, 76%); **HRMS** (ESI +ve) calcd for $C_{29}H_{28}N_5O_4^+$ 510.21413 found 510.21405.

***N*-(3-(9,10-dioxo-9,10-dihydroanthracen-1-ylamino)propyl)-1-methyl-4-(1-methyl-4-(1-methyl-1*H*-pyrrole-2-carboxamido)-1*H*-pyrrole-2-carboxamido)-1*H*-pyrrole-2-carboxamide (3py-1C3) 4c**

The peptide coupling of methylpyrrole polyamide carboxylic acid (0.143 g, 0.39 mmol, 1.0

eq) and 1C3 **2** (0.131g, 0.47 mmol, 1.2 eq) followed general procedure A. The residue was purified using flash column chromatography (EtOAc, R_F 0.44) yielding **4c** (0.154g, 63%) as a red solid; **M.p** 144-145 °C; **IR** (ATR) 3355, 3009, 2911, 1632, 1591, 1511, 1406, 1271 cm^{-1}; **^{1}H NMR** (400 MHz, $CDCl_3$) δ 9.72-9.82 (1H, m), 8.17-8.25 (2H, m), 7.60-7.75 (3H, m), 7.56-7.60 (1H, m), 7.49-7.56 (1H, m), 7.36-7.40 (1H, m), 7.10-7.12 (1H, m), 7.05-7.09 (1H, m), 7.03-7.05 (1H, m), 6.75-6.77 (1H, m), 6.66-6.69 (1H, m), 6.61-6.63 (1H, m), 6.42-6.46 (1H, m), 6.10-6.18 (2H, m), 3.97 (3H, s), 3.90 (3H, s), 3.86 (3H, s), 3.52-3.60 (2H, m), 3.40-3.48 (2H, m), 2.00-2.10 (2H, m); **^{13}C NMR** (100 MHz, $CDCl_3$) δ 184.4, 183.5, 162.0, 159.4, 158.9, 151.1, 134.9, 134.5, 134.0, 133.9, 133.7, 132.7, 132.5, 128.4, 126.3, 125.2, 123.0, 122.7, 121.6, 121.4, 119.5, 119.1, 117.6, 115.6, 112.4, 112.2, 107.3, 103.7, 103.4, 40.3, 37.0, 36.7, 36.6, 36.5, 28.9; **MS** (ESI +ve) m/z 632.1 ($M+H^+$, 69%), 654.5 ($M+Na^+$, 40%); **HRMS** (ESI +ve) calcd for $C_{35}H_{33}N_7NaO^+$ 654.24354 found 654.24368.

1,5-di((aminopropyl)amino)anthraquinone (1,5C3) 3

A solution of propane-1,3-diamine (34 mL, 407 mmol, 20.0 eq) in anhydrous MeCN (180 mL) was heated at reflux and 1,5-dichloroanthraquinone (6 g,21.7 mmol, 1.0 eq) was added slowly as a solid to the refluxing mixture which was then heated at reflux for 3 days. The solution was removed under reduced pressure and the residue was resuspended in chloroform (400 mL). Water was added and the aqueous phase was acidified using HCl (1 M) until pH 1 was reached and washed using chloroform (3 × 400 mL). NaOH (1 M) was added to the aqueous layer until pH 10 was reached and extracted with chloroform (6 × 250 mL). The combined organic extracts were dried (Na_2SO_4) and the solvent removed under reduced pressure. The residue was purified by alumina chromatography and the red band collected yielding **3** (5.62g, 74%) as a dark red solid. **M.p.** 171-173 °C; **IR** (ATR) 3359, 3280, 2944, 2890, 2861, 1618, 1572, 1508, 1258 cm^{-1}; **^{1}H NMR** (400 MHz, $CDCl_3$) δ 9.72 (2H, m), 7.48-7.56 (4H, m), 6.99 (2H, dd, *J* 8.0, 1.6 Hz), 3.40 (4H, q, *J* 5.8 Hz), 2.91 (4H, t, *J* 5.8 Hz), 1.90 (4H, pentet, *J* 6.3 Hz), 1.48 (6H, br s); **^{13}C NMR** (100 MHz, $CDCl_3$) δ 185.4, 151.4, 136.2, 135.1, 116.3, 114.7, 112.9, 40.4, 39.7, 32.7; **MS** (ESI +ve) m/z 353.3 ($M+H^+$, 100%), 705.2 ($2M+H^+$, 40%); **HRMS** (ESI +ve) calcd for $C_{20}H_{25}N_4O_2^+$ 353.19720 found 353.19759.

***N*-(3-(5-(3-Aminopropylamino)-9,10-dioxo-9,10-dihydroanthracen-1-ylamino)propyl)-1-methyl-1*H*-pyrrole-2-carboxamide (1py-1,5C3) 5a**

The peptide coupling of methylpyrrole carboxylic acid **9** (31 mg, 0.24 mmol, 1.0 eq) and

1,5C3 3 (3.0 eq) followed general procedure A'. The residue was purified by silica chromatography (1:9 v/v, MeOH/chloroform, R_F 0.12) yielding **5a** as a dark hygroscopic purple solid (100 mg, 87%); **IR** (ATR) 3362, 2915, 1679, 1253cm^{-1}; **^{1}H NMR** (300 MHz, MeOD) δ 7.43-7.60 (4H, m), 7.05-7.14 (2H, m), 6.75-6.79 (1H, m), 6.70-6.74 (1H, m), 5.99-6.04 (1H, m), 3.86 (3H, s), 3.38-3.54 (6H, m), 3.06-3.16 (2H, m), 1.94-2.14 (4H, m); **^{13}C NMR** (100 MHz, MeOD) δ 186.6, 186.0, 164.6, 152.5, 152.2, 137.4, 137.1, 136.4, 136.2, 129.1, 126.7, 117.8, 117.4, 116.1, 115.6, 114.2, 113.7, 108.0, 41.3, 40.3, 38.5, 38.0, 36.6, 30.2, 28.1; **MS** (ESI +ve) m/z 804 (M+H$^+$, 55%).

_N_-(3-(5-(3-aminopropylamino)-9,10-dioxo-9,10-dihydroanthracen-1-ylamino)propyl)-1-methyl-4-(1-methyl-1_H_-pyrrole-2-carboxamido)-1_H_-pyrrole-2-carboxamide (2py-1,5C3) 5b

The peptide coupling of methylpyrrole polyamide carboxylic acid **11** (217 mg, 0.88 mmol, 1.0 eq) and **1,5C3 3** (927 mg, 2.63 mmol, 3.0 eq) followed general procedure A'. The residue was purified using silica chromatography (9:90:1 v/v/v, MeOH/chloroform/TEA, R_F 0.24) yielding **5b** (160 mg, 31%) as a dark hygroscopic purple solid; **IR** (ATR) 3326, 2972, 2925, 1667, 1596, 1505, 1253, 1043 cm^{-1}; **^{1}H NMR** (300 MHz, DMSO-d$_6$) δ 9.60-9.80 (4H, m), 8.10-8.20 (1H, m), 7.55-7.70 (2H, m),7.40-7.48 (2H, m), 7.12-7.20 (2H, m), 7.08-7.15 (1H, m), 6.92-6.95 (1H, m), 6.88-6.92 (2H, m), 6.00-6.10 (1H, m), 4.32 (2H, br s), 3.84 (3H, s), 3.77 (3H, s), 3.40-3.60 (2H, m), 2.80-3.00 (2H, m), 1.80-2.00 (6H, m), 1.10-1.30 (2H, m); **^{13}C NMR** (75 MHz, DMSO-d$_6$) δ 161.8, 158.9, 151.4, 151.2, 135.9, 128.4, 125.9, 123.3, 122.8, 122.4,118.4, 118.2, 117.4, 114.6, 112.9, 111.7, 107.0, 104.7, 62.4, 36.6, 36.3, 29.3, 25.8, peaks obscured by DMSO-d$_6$ peaks (δ 39.0-40.8); **MS** (ESI +ve) m/z 582 (M+H$^+$, 100%); **HRMS** calcd for $C_{32}H_{36}N_7O_4^+$ 582.28233, found 582.28088.

_N_-(3-(5-(3-aminopropylamino)-9,10-dioxo-9,10-dihydroanthracen-1-ylamino)propyl)-1-methyl-4-(1-methyl-4-(1-methyl-1_H_-pyrrole-2-carboxamido)-1_H_-pyrrole-2-carboxamido)-1_H_-pyrrole-2-carboxamide (3py-1,5C3) 5c

The peptide coupling of methylpyrrole polyamide carboxylic acid (239 mg, 0.65 mmol, 1.0 eq) and 1,5C3 **3** (684 mg, 1.94 mmol, 3.0 eq) followed general procedure A'. The residue was purified using silica chromatography (9:90:1 v/v/v, MeOH/chloroform/TEA, R_F 0.48) yielding **5c** as a dark hygroscopic purple solid (105 mg, 23%); **IR** (ATR) 3305, 3280, 2918,

2850, 1617, 1506, 1253 cm^{-1}; **^{1}H NMR** (400 MHz, DMSO-d_6) δ 9.87-9.91 (1H, m), 9.81-9.86 (1H, m), 9.64-9.76 (2H, m), 8.13-8.20 (1H, m), 7.74-7.79 (1H, m), 7.60-7.69 (2H, m), 7.54-7.7.58 (1H, m), 7.41-7.50 (2H, m), 7.25-7.30 (1H, m), 7.22-7.25 (1H, m), 7.15-7.20 (2H, m), 7.02-7.06 (1H, m), 6.91-6.96 (2H, m), 6.04-6.08 (1H, m), 3.87 (3H, s), 3.84 (3H, s), 3.80 (3H, s), 2.89-2.94 (10H, m), 1.81-1.97 (4H, m); **^{13}C NMR** (100 MHz, DMSO-d_6) δ 184.8, 184.6, 161.9, 159.1, 158.9, 151.5, 151.3, 143.4, 136.1, 135.9, 128.6, 127.8, 125.9, 124.6, 123.6, 123.4, 122.6, 122.6, 118.9, 117.5, 115.0, 114.7, 113.2, 112.6, 112.4, 111.1, 107.1, 104.8, 37.2, 36.6, 36.5, 31.5, 29.4, 27.1, peaks obscured by DMSO-d_6 peak; **MS** (ESI +ve) m/z 704 ($M+H^+$, 100%); **HRMS** calcd for $C_{38}H_{41}N_9O_5^+$ 704.33034, 705.33358, 706.33699 found 704.33006, 705.33316, 706.33690.

Chlorido(ethane-1,2-diamine)((1- (propylamine)anthraquinone) propioamidine)platinum(II) chloride, [PtCl(am1C3)(en)]Cl 7

The conjugation of 1C3 **2** (16.6 mg, 59.0 µmol, 1.0 eq) and [PtCl(en)(NCEt)]Cl **6** (22.5 mg, 59.0 µmol, 1.0 eq) followed general procedure D yielding a red solid **7** (16.0 mg, 41%); **^{1}H NMR** (400 MHz, DMF-d_7) δ 9.70-9.85 (1H, m), 8.20-8.30 (1H, m), 8.07-8.20 (1H, m), 7.80-7.95 (2H, m)-, 7. 0-7.75 (1H, m), 7.35-7.53 (2H, m), 3.40-3.5 (2H, m), 2.75-2.90 (2H, m), 2.60-2.70 (4H, m), 1.95-2.10 (2H, m), 1.35- 1.45 (2H, m); **^{195}Pt NMR** (86 MHz, DMF-d_7) δ -2481; **MS** (ESI +ve) m/z 624 (74%), 625 (100%), 628 (50%), 629 (14%); **HRMS** (ESI +ve) calcd for $C_{22}H_{29}{}^{35}ClN_5O_2Pt^+$ 624.16309, 625.16537, 626.16523, 627.16255, 628.16274, 629.16583, 630.16537 found 624.16373, 625.16565, 626.16584, 627.16481, 628.16542, 629.16915, 630.16586.

Chlorido(ethane-1,2-diamine)((1-(1-*N*-methylpyrrole-2-carboxamidopropylamine),5-(propylamine)anthraquinone) propioamidine)platinum(II) chloride, [PtCl(am(1py-1,5C3))(en)]Cl 8

The conjugation of **1py-1,5C3 4b** (56.8 mg, 0.12 mmol, 1.0 eq) and [PtCl(en)(NCEt)]Cl **6** (45.7 mg, 0.12 mmol, 1.0 eq) followed general procedure D yielding **8** as a pink solid (58.9 mg, 58%); **IR** (ATR) 3283, 3204, 1597, 1568, 1504, 1259, 1194, 1128, 1053, 765, 575 cm^{-1}; **^{1}H NMR** (400 MHz, DMF-d_7) δ 9.60-9.75 (2H, m), 8.0-8.15 (2H, m), 7.53-7.70 (2H, m), 7.35-7.50 (2H, m), 7.10-7.25 (3H, m), 6.90 (1H, br s), 6.70-6.80 (1H, m), 5.95-6.00 (1H, m), 3.82 (3H, s), 3.28-3.33 (4H, m), 3.00-3.10 (5H, m), 1.80- 1.90 (4H, m); **^{195}Pt NMR**

(86 MHz, DMF-d_7) δ -2324; **^{13}C NMR** (100 MHz, DMF-d_7) δ 184.4, 184.3, 161.8, 151.1, 135.8, 127.8, 125.8, 117.6, 114.7, 112.2, 112.0, 106.7, 79.5, 57.9, 49.1, 47.6, 45.7, 36.3, 29.1, 12.5, 8.5, 7.8; **MS** (ESI +ve) m/z 803 (69%), 804 (95%), 805 (100%), 806 (57%), 807 (41%); **HRMS** (ESI +ve) calcd for $C_{31}H_{42}{}^{35}ClN_8O_3Pt^+$ 803.26895, 804.27127, 805.27117, 806.26852, 807.26864, found 803.26951, 804.27268, 805.27202, 806.27363, 807128.

Chlorido(ethane-1,2-diamine)((1-(2-*N*-methylpyrrole-2-carboxamidopropylamino),5-(propylamine)anthraquinone)propioamidine) platinum(II) chloride, [PtCl(am(2py-1,5C3))(en)]Cl 9

The conjugation of **2py-1,5C3 5b** (34.8 mg, 59.8 µmol, 1.0 eq) and [PtCl(en)(NCEt)]Cl **6** (22.8 mg, 59.8 µmol, 1.0 eq) followed general procedure D yielding **9** as a pink solid (23.0 mg, 40%); **IR** (ATR) 3284, 1598, 1512, 1401, 1258, 1189, 1130, 1053, 768, 575 cm^{-1}; **^{1}H NMR** (400 MHz, DMF-d_7) δ 9.99 (1H, br s), 9.65-9.80 (2H, m), 8.32 (1H, br s), 7.60-7.70 (1H, m), 7.40-7.55 (2H, m), 7.32-7.35 (1H, m), 7.13-7.30 (3H, m), 7.05- 7.13 (2H, m), 6.90-7.00 (1H, m), 6.12 (1H, br s), 6.04 (1H, br s), 3.97 (3H, s), 3.92 (3H, s), 2.93-2.96 (1H, m), 2.80-2.92 (2H, m), 2.75-2.82 (2H, m), 2.72-2.75 (3H, m), 2.65-2.72 (2H, m), 2.60-2.65 (4H, m), 1.90-2.10 (4H, m); **^{13}C NMR** (100 MHz, DMF-d_7) δ 185.0, 173.0, 172.1, 170.0, 168.5, 166.4, 162.7, 162.1, 160.4, 159.4, 151.7, 142.6, 136.3, 130.6, 129.4, 128.5, 127.5, 126.2, 124.7, 123.8, 23.2, 119.7, 119.2, 118.4, 117.5, 114.8, 112.8, 107.0, 104.5, 90.2, 87.8, 49.8, 40.7, 39.3, 37.0, 36.5, 35.9, 34.5, 30.7, 29.7, 25.7, 12.5, 11.3; **^{195}Pt NMR** (86 MHz, DMF-d_7) δ -2307; **MS** (ESI +ve) m/z 927 (M^+, 100%); **HRMS** (ESI +ve) calcd for $C_{37}H_{48}ClN_{10}O_4Pt^+$ 925.31696, 926.31930, 927.31923, 928.31659, 929.31668 found 925.31876, 926.32077, 927.32223, 928.31944, 929.31803.

Chlorido(ethane-1,2-diamine)((1-(3-*N*-methylpyrrole-2-carboxamidopropylamine),5-(propylamine)anthraquinone) propioamidine)platinum(II) chloride, [PtCl(am(3py-1,5C3))(en)]Cl 10

The conjugation of **3py-1,5C3 23** (47.1 mg, 66.9 µmol, 1.0 eq) and [PtCl(en)(NCEt)]Cl **6** (25.2 mg, 66.9 µmol, 1.0 eq) followed general procedure D yielding **10** as a dark red solid (16.9 mg, 22%); **IR** (ATR) 3214, 1635, 1597, 1507, 1457, 1405, 1258, 1188, 1115, 1075, 804, 771, 517 cm^{-1}; **^{1}H NMR** (400 MHz, DMF-d_7) δ 10.00-10.20 (1H, m), 9.60-9.80

(1H, m), 7.60-7.70 (1H, m), 7.40-7.55(2H, m), 7.35-7.40 (2H, m), 7.20-7.30 (2H, m), 7.05-7.20 (2H, m), 6.95-7.00 (1H, m), 6.40-6.47 (1H, m), 6.00-6.07 (1H, m), 5.60-5.70 (1H, m), 3.98 (3H, s), 3.95 (3H, s), 3.91 (3H, s), 2.60-2.70 (3H, m), 2.05-2.25 (2H, m), 1.80-2.05 (2H, m), 1.00-1.35 (4H, m); **^{195}Pt NMR** (86 MHz, DMF-d_7) δ -2541; **MS** (ESI +ve) m/z 1049 (M^+, 100%); **HRMS** (ESI +ve) calcd for $C_{43}H_{54}ClN_{12}O_5Pt^+$ 1047.36498, 1048.36733, 1049.36728, 1050.37022, 1051.36473, 1052.36778, 1053.36730 found 1047.36611, 1048.36773, 1049.36762, 1050.36867, 1051.36932, 1052.37033, 1053.37353.

Experiments with human cells

The cytotoxicity studies were performed using cisplatin as a reference compound. MTT (3-[4,5-dimethylthiazol-2-yl]-2,5-diphenyltetrazolium bromide) was purchased from Sigma Aldrich. The organic compounds were dissolved in DMSO and the platinum complexes were dissolved in DMF just before the experiment and an aliquot of the solution was added to the growth medium (final concentration ranging between 0 to 200 μM) containing the cells. The carrier solvent never exceeded 1% of the growth medium and had no discernible effect on cell viability.

Cell cultures

Human colon (DLD-1) and breast (MDA-MB-231) carcinoma cell lines were obtained by American Type Culture Collection (ATCC, Rockville, MD). The cell lines were cultured as monolayers in a plastic treated sterile flask in Advanced DMEM, supplemented with 2% foetal calf serum (FCS) and 1% glutamine. The cells were incubated at 37 °C, with 5% CO_2 under humidified conditions. The monolayer cells were sub-cultured when the layers became 70-80% confluent, using 0.25% trypsin at 37 °C for cell dissociation from the flask.

Cytotoxicity assay (MTT assay)

The growth inhibitory effect against the carcinoma cell lines was evaluated by the use of the MTT assay. The method involved seeding 1×10^4 cells in 100 μL of growth medium (2% FCS, 1% glutamine) in a 96-well plate and allowing them to adhere overnight in an incubator. The growth medium in the wells that was used for seeding the cells was removed and 100 μL aliquots of the assigned drug concentrations were added in triplicate to the wells. The cells were then incubated for 72 h at 37 °C, with 5% CO_2 under humidified conditions. A 1 mM final concentration of MTT (20 μL) was added to each well and the cells were incubated for a further 4 h. The growth medium was removed and DMSO (150 μL) was

added to dissolve the purple formazan crystals. The 96-well plates were shaken until the solutions were uniform. The absorbance of the plate at 600 nm was then read using a Victor microplate reader from Perkin Elmer. The mean absorbance for each drug dose was calculated and plotted against the drug concentration. The IC_{50} values were determined by the concentration of drug at which the absorbance value was half the absorbance value of the cells grown in untreated control wells.

Subcellular distribution studies

Monolayers (DLD-1, 1.5 x 10^4 cells; MDA-MB-231, 2.5 x 10^4 cells) were incubated on MatTek dishes overnight (typically 12-16 h). Compounds were added to the cells (10 μM) and incubated for 4 h, followed by the addition of Hoechst 33358 (2 μM) to the dish 3 min prior to imaging. The fluorescent compounds were detected using an Olympus Fluoview FV1000 inverted light, fluorescence a confocal microscope. Hoechst 33358 was excited with a LD405 nm visible laser. The compounds **2, 3, 4a-c, 5a-c** were all excited at $\lambda = 559$ nm with an emission filter set for $\lambda > 570$ nm.

Cellular accumulation studies

Approximately 1×10^6 DLD-1 or MDA-MB-231 cells were seeded onto 3.5 cm^3 dishes and allowed to adhere for 16 h. The cells were incubated with the compounds (10 μM) for 24 h. The cells were harvested by incubation with trypsin (1 mL, 5 min), followed by the inactivation of trypsin by the addition of Adv DMEM (1 mL). The cell pellet was washed 3 times with PBS and then resuspended in PBS (0.5 mL). Aliquots were taken from the cell sample for protein analysis (100 μL) and platinum analysis (100 μL). The samples were stored at -20 °C until immediately prior to analysis. All experiments were repeated at least three times.

Sample preparation for GF-AAS involved the digestion of the cell samples (100 μL) with HNO_3 (69%, AAS grade, 200 μL). The mixture was sonicated in an ultrasonic bath for 2 h. The digested samples were diluted with MilliQ water (200 μL) before GF-AAS analysis. The obtained platinum concentrations were normalised against the cellular protein concentrations determined by the protein assay.

Protein assay

Protein concentrations were determined using the Biorad protein assay [34]. The binding of protein to the Coomassie Brilliant Blue G-250 reagent shifts the absorbance from 465 to 595 nm. The Biorad reagent was diluted 1 in 5 with MilliQ water immediately prior to use. MilliQ water (400 µL) was added to each 100 µL aliquot of cell solution. Standard protein solutions (0, 0.05, 0.1, 0.2, 0.3, 0.4, 0.45, 0.5 mg/mL) were prepared from bovine serum albumin (in PBS) and stored at 4 °C prior to use. Cell samples were placed in an ultrasonic bath for 1 h, followed by vigorous mixing prior to being assayed.

The protein assay was carried out by adding the diluted Biorad reagent (150 µL per well) into the wells of a 96-well plate. Aliquots (10 µL) of the standard protein solutions were added to the Biorad reagent. The cell samples treated with the platinum complexes were added to the Biorad reagent in triplicate. The protein/dye mixtures were shaken for 3 min and were allowed to stand at rt for 10 min. The absorbance of each well was measured at 600 nm. The protein concentrations of the cell samples were determined using the absorbance standard curve established from the protein standard solutions.

HRE-EosFP spheroid studies

Spheroids were prepared from HRE-EosFP transfected DLD-1 cells. The wells of a 96-well plate were coated with hot sterile 0.8% (w/v) agarose in PBS (35 µL) and left to solidify at rt for 20 to 30 min. The agarose coated wells were seeded with 1.5 x 10^4 cells per well in 100 µL of supplemented medium. The seeded cells were incubated at 37 °C at 5% CO_2 for 96 h to allow for cell-cell aggregation. These conditions were optimised by Kim *et al.* and this protocol was used to make the spheroids [35]. Medium (15K cells) sized spheroids were chosen since they were large enough to form a hypoxic region that could be visualised *via* the green fluorescent protein [35]. The spheroids formed were consistently between 500-600 µm in diameter.

Fluorescence distribution studies in HRE-EosFP yransfected DLD-1 spheroids

The fluorescence distributions in 15K spheroids made from HRE-EosFP transfected DLD-1 carcinoma cells were imaged after dosing with **2, 3, 4a-c**, **5a-c** and platinum(II) complexes **7, 8a-c** (10 µM) for 24 h. The averaged fluorescence profiles were compiled for comparison of the penetrative ability of the compounds in tumour spheroid models.

Acknowledgments This research was undertaken at the cell culture laboratory at the Australian Microscopy and Micro-Analysis Research Facility (AMMRF) at the University of Sydney, NSW, Australia

Abbreviations Ascorbate, L-ascorbate; dma, dimethylamine; ipa, isopropylamine; OAc, Acetate; OPr, Propionate; py, pyridine; DMF, dimethylformamide; DMA, dimethylacetamide; DMSO, dimethyl sulfoxide; ox, oxalate; en, ethane-1,2-diamine; rt, room temperature.

Compliance with ethical standards

Conflicts of Interest The authors declare no conflict of interest.

References

1 L. R. Kelland (2007) Nat Rev Cancer 7:573-584
2 I. S. Um, E. Armstrong-Gordon, Y. E. Moussa, D. Gnjidic and N. J. Wheate (2019) Inorganica Chimica Acta 492:177-181
3 N. J. Wheate, S. Walker, G. E. Craig and R. Oun (2010) Dalton Transactions 39:8113-8127
4 T. W. Hambley (2019) J Biol Inorg Chem 24:457-466
5 M. Srinivasarao, C. V. Galliford and P. S. Low (2015) Nat Rev Drug Discov 14:203-219
6 J. Woynarowski, W. Chapman, C. Napier and M. Herzig (1999) Biochim Biophys Acta 1444:201-217
7 J. Woynarowski, C. Napier, A. Trevino and B. Arnett (2000) Biochemistry 39:9917-9927
8 Z. Ma, J. R. Choudhury, M. W. Wright, C. S. Day, G. Saluta, G. L. Kucera and U. Bierbach (2008) Journal of Medicinal Chemistry 51:7574-7580
9 C. L. Smyre, G. Saluta, T. E. Kute, G. L. Kucera and U. Bierbach (2011) ACS Med Chem Letters 2:870-874
10 U. Ellervik, C. C. C. Wang and P. B. Dervan (2000) J Am Chem Soc 122:9354-9360
11 S. White, J. W. Szewczyk, J. M. Turner, E. E. Baird and P. B. Dervan (1998) Nature 391:468-471
12 R. I. Taleb, D. Jaramillo, N. J. Wheate and J. R. Aldrich-Wright (2007) Chem - Eur J 13:3177-3186
13 D. Jaramillo, N. J. Wheate, S. F. Ralph, W. A. Howard, Y. Tor and J. R. Aldrich-Wright (2006) Inorg Chem 45:6004-6013
14 E. J. Fechter and P. B. Dervan (2003) J Am Chem Soc 125:8476-8485
15 E. J. Fechter, B. Olenyuk and P. B. Dervan (2004) Angewandte Chemie-International Edition 43:3591-3594

16 A. Eliadis, D. R. Phillips, J. A. Reiss and A. Skorobogaty (1988) Journal of the Chemical Society-Chemical Communications, doi 10.1039/c39880001049:1049-1052
17 L. Supekova, J. P. Pezacki, A. I. Su, C. J. Loweth, R. Riedl, B. Geierstanger, P. G. Schultz and D. E. Wemmer (2002) Chem Biol 9:821-827
18 Y. Hiraku, S. Oikawa, S. Kawanishi, H. Sugiyama and I. Saito (1999) Nucleic acids symposium series:253-254
19 A. I. Minchinton and I. F. Tannock (2006) Nat Rev Cancer 6:583-592
20 N. S. Bryce, J. Z. Zhang, R. M. Whan, N. Yamamoto and T. W. Hambley (2009) Chem Commun in press:2673-2675
21 S. Ding, X. Qiao, G. L. Kucera and U. Bierbach (2012) J Med Chem 55:10198-10203
22 J. Z. Zhang, N. S. Bryce, A. Lanzirotti, C. K. J. Chen, D. Paterson, M. D. de Jonge, D. L. Howard and T. W. Hambley (2012) Metallomics 4:1209-1217
23 A. Z. M. Pauzi, S. K. Yeap, N. Abu, K. L. Lim, A. R. Omar, S. A. Aziz, A. L. T. Chow, T. Subramani, S. G. Tan and N. B. Alitheen (2016) Chin Med 11:11
24 G.-J. Zhao, and K.-L. Han (2008) In: A. Sánchez, and S. J. Gutierrez (ed) Photochemistry Research Progress. Nova Science Publishers, pp. 161-190
25 T. Yatsuhashi and H. Inoue (1997) J Phys Chem A 101:8166-8173
26 B. A. J. Jansen, P. Wielaard, G. V. Kalayda, M. Ferrari, C. Molenaar, H. J. Tanke, J. Brouwer and J. Reedijk (2004) J Biol Inorg Chem 9:403-413
27 R. Whan (2007) PhD Thesis, School of Chemistry. The University of Sydney,
28 R. A. Alderden, H. R. Mellor, S. Modok, T. W. Hambley and R. Callaghan (2006) Biochem Pharmacol 71:1136-1145
29 A. Glenister, M. I. Simone and T. W. Hambley (2019) PLoS One 14
30 A. Lo , V. Murray and T. W. Hambley (2020) tbd,
31 A. T. S. Lo, N. K. Salam, D. E. Hibbs, P. J. Rutledge and M. H. Todd (2011) Plos One 6:e17446
32 R. M. Whan, B. A. Messerle and T. W. Hambley (2009) Dalton Trans, doi 10.1039/b814604g:932-939
33 J. Katzhendler, K. F. Gean, G. Barad, Z. Tashma, R. Benshoshan, I. Ringel, U. Bachrach and A. Ramu (1989) Eur J Med Chem 24:23-30
34 H. Burger, A. Zoumaro-Djayoon, A. W. M. Boersma, J. Helleman, E. Berns, R. H. J. Mathijssen, W. J. Loos and E. A. C. Wiemer (2010) British Journal of Pharmacology 159:898-908
35 B. J. Kim, T. W. Hambley and N. S. Bryce (2011) Chem Sci 2:2135-2142

Table of Contents Entry

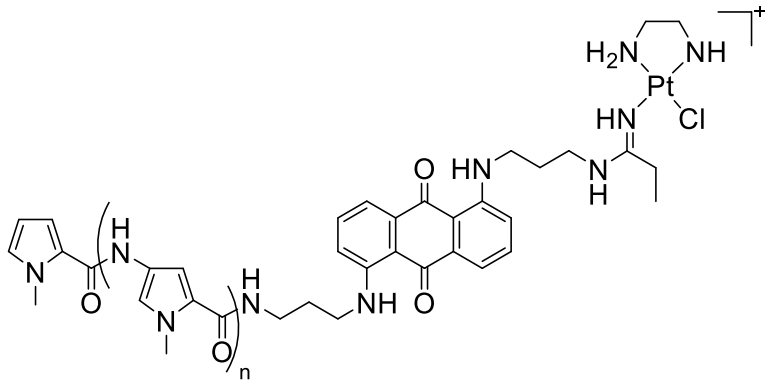

Trifunctional DNA binding complexes consisting of monofunctional platinum binder, an intercalator and an minor groove binding polypyrolle have been investigated as possible anticancer entities.